Order parameters of α,ω-diphenylpolyenes in a nematic liquid crystal from an integrated computational and ^{13}C NMR spectroscopic approach

Caterina Benzi[a*], Vincenzo Barone[a], Riccardo Tarroni[b] and Claudio Zannoni[b]

(a) Dipartimento di Chimica and INSTM, Università Federico II, Complesso Monte S. Angelo, via Cintia, I-80126 Napoli, Italy;

(b) Dipartimento di Chimica Fisica ed Inorganica and INSTM, Università di Bologna, viale Risorgimento 4, I-40136 Bologna, Italy

Abstract

The orientational order parameters and conformational behavior of five relatively large rod-like molecules, biphenyl, trans-stilbene, 1,3-diphenyl-butadiene, 1,3,5-diphenyl-hexatriene and 1,3,5,7-diphenyl-octatetraene, dissolved in the thermotropic liquid crystal ZLI-1167, have been studied using an integrated approach combining ^{13}C NMR measurements and quantum mechanical computations of carbon chemical shift tensors. Besides biphenyl, the phenyl moiety of all structures has been found to have an high rotational mobility in the temperature range of the present experiments. The rank-two order parameter $\langle P_2 \rangle$ in the nematic phase is found to increase steadily from the shortest to the longest term of the series, at any temperature within the nematic range. The molecular biaxiality order parameter $\langle D^2_{02} \rangle$ is found to be small and essentially constant with temperature, giving further support to the common assumption of effective uniaxiality for these probes.

---

*Corresponding author: e-mail: catbenzi@unina.it; phone: +39 081 674204; fax: +39 081 674090

1 Introduction

In recent years, there has been an increasing interest in investigating the relationship between the observable properties of liquid crystals [1] (first of all the orientational order,[2,3]) and their molecular structure and intermolecular interactions. Both theoretical and experimental techniques have been employed to establish a link between macroscopic and microscopic features, stimulated by the continuing interest in the possible technological applications,[4] and by the aim of designing compounds leading to ordered materials having specifically tailored properties.

In this context the accurate determination of orientational order parameters for molecules with well defined properties (symmetry, rigidity, aspect ratio etc.) and systematically increasing complexity, plays a key role and a variety of techniques have been employed for the purpose.[1] Amongst spectroscopic techniques Nuclear Magnetic Resonance (NMR) plays an especially important role, thanks to the well defined relation existing between spectral data and single molecule ordering properties, which allows an unambiguous interpretation of the experimental data.[5] NMR collects a family of techniques among which proton (H-NMR) and deuterium (D-NMR) have been particularly used for this purpose. However, both these approaches present limitations. ^{1}H NMR is severely limited to the number of coupled spins present in the molecule, and as far as we are aware, biphenyl is still the largest molecule studied. On the other hand, D-NMR has the obvious limitation of requiring a isotopic substitution synthetic stage, which complicates or makes it impossible the study of a planned series of molecules. Among other NMR techniques, natural abundance carbon-13 Nuclear Magnetic Resonance (^{13}C-NMR) studies of mesogen molecules or probe molecules dissolved in mesophases are gaining increasing popularity, [6−11] due to the improvements both in solid-state techniques [10,11] and in ab-initio shielding-tensor calculation methods.[12,13] Indeed, in recent years, the quantum mechanical (QM) calculation of magnetic properties of small to medium size organic and biological molecules[14,18] has reached high standards, and has become a valuable tool for the interpretation of spectra while providing a deeper understanding of the effects influencing the magnetic behavior of such systems. In particular, high-level QM calculations of chemical shielding constants and effective descriptions of

the environment surrounding the molecule have given further insights on conformation and on short- and long- range interactions.[14−15] Methods rooted in Density Functional Theory[16] (DFT) are particularly appealing since they couple remarkable accuracy with a favorable scaling with the number of active electrons, and their integration with continuum solvent models like the Polarizable Continuum Model[17] (PCM) well reproduces solvent effects on the magnetic properties.[18] The recently-developed approach allowing for anisotropic solutions[19] made the calculation of chemical shielding tensors feasible also for molecules dissolved in a partially ordered environment.[20]

In evaluating structural and environmental effects, the advantages gained from the use of chemical shielding tensors instead of isotropic chemical shieldings (defined as one-third of the trace of the corresponding shielding tensors) stem from an increased sensitivity to the surroundings of the nuclei. In fact, the directional properties of the tensor are associated with the nuclei's three dimensional electronic environment, which is in turn affected by the chemical structure and by solvent anisotropies. Part of this information may be accidentally lost when isotropic shieldings are employed.

Solid-state NMR can now provide chemical shielding tensors with an high degree of accuracy: nevertheless, a direct, unambiguous relation between chemical shieldings and molecular structure is difficult to be achieved, and therefore a theoretical approach is needed as a link between the experimental observable and the structural information lying behind it: this approach has been successfully used for conformational analysis of peptides [21] and organic molecules.[22] Due to the increasing popularity of these methods, a considerable number of methodological studies have been devoted to either improve the accuracy of chemical shielding tensor DFT calculations[13] or to reduce the computational effort as the number of atoms in the molecular system[23] increases.

In this work, we couple our expertise in partially ordered condensed phases with highly accurate chemical shielding tensor calculations and use this approach to determine magnetic tensors of ^{13}C nuclei of diphenylpolyenes dissolved in liquid crystals. In a previous study,[20] we have tested the use of computed chemical shieldings as input data for the determination of the orientational behavior of some rigid organic molecule dissolved in a thermotropic liquid crystal, whose order parameters are known from

^{2}H-NMR results. We now extend, refine and validate this method to the study of more complicated molecules whose usefulness in determining order and dynamics in anisotropic phases is well established. We focus our attention to an homologous series of α,ω-diphenylpolyenes dissolved in the thermotropic liquid crystal ZLI-1167.[24,25] Order parameters are determined as a function of temperature, starting from ^{13}C experimental spectra and computed tensors: the high accuracy obtained proves that accurate and time consuming experimental information about the ^{13}C shielding tensors may be safely substituted by computed data.[26–28] Moreover, an analysis of the dependence of the magnetic properties from the molecular structure has been performed. Diphenylpolyenes represent a class of molecules with peculiar photophysical and photochemical properties that make them particularly interesting and suitable as fluorescent probes for liquid crystals and membrane interior [31] as well as prototypes of more complex systems such as carotenoids and polyacetylenes.[32] In particular 1,6-diphenyl-hexatriene (DPH) is certainly the most widespread fluorescent probe used in ordered systems, such as liquid crystals and membrane bilayers.[31,33] To the best of our knowledge, ^{2}H-NMR techniques have been applied only to DPH,[34] and this lack of experiments may be attributed to the the additional complications of synthesizing deuterated diphenyl-polyenes.

Using a ^{13}C-NMR technique, we succeeded in studying a whole series of structurally related probes in the same thermotropic liquid crystal solvent, using commercial chemicals and instrumentations. The lack of solid state information about the carbon shielding tensors of these molecules is effectively overcome with the use of high-level quantum mechanical computations. In the following sections the data analysis model will be outlined, as well as the experimental and computational methods. The computed chemical shielding tensors and the ^{13}C order parameters for all the set of diphenyl-polyenes will then be presented. We believe this is the first case where a detailed study of the orientational order and of its biaxiality for molecules of this complexity is presented and we trust it will be of help in developing more realistic theories of solute ordering in liquid crystals.

2 Methods

2.1 Experimental

Biphenyl (BP), trans-stilbene (diphenylethylene, DPE), all-trans 1,3-diphenyl-butadiene (DPB), all-trans 1,3,5-diphenyl-hexatriene (DPH), and all-trans 1,3,5,7-diphenyl-octatetraene (DPO) were purchased from Aldrich and used without further purification. The liquid crystal ZLI-1167, a ternary eutectic mixture of 4′-propyl, 4′-pentyl and 4′-heptyl-4-cyanobicyclohexyls,[25] was purchased from Merck. This saturated solvent is particularly useful to study aromatic solutes, like in our case, since the solute and solvent bands are well separated after proton decoupling.

The temperature dependent series of ^{13}C NMR spectra were recorded on a Bruker CXP 300 Pulse Spectrometer, using the same single pulse technique and experimental setup described in detail in Ref. 26, where we also discuss the precautions taken to avoid RF heating. All the spectra were recorded in a single temperature sweep, cooling from isotropic (355 K) to about room temperature (307 K), thus minimizing the experimental artifacts and making unnecessary the use of tetramethylsilane as reference. We used instead, as internal reference, the carbon of the cyano group of the liquid crystal. A selection of spectra is shown in figure 1.

Each sample, prepared by dissolving the molecular probe into the liquid crystal at approximately 3% w/w weight ratio, was sealed in a NMR tube 8 mm diameter. All probes, excepted DPO, dissolve completely at this concentration. At least 400 scans were accumulated for each temperature. Due to its low solubility in the mesophase, up to 2000 scans were required for DPO to get a good s/n ratio.

In figs.2-6 we show the observed chemical shifts, the carbon labellings, and the line assignments both in the isotropic and in the nematic phase. For the isotropic line assignments, we essentially used literature data,[35−37] while for the assignments in the mesophase we applied the trial-and-error procedure described in previous works.[26−28]

For DPE, DPB, DPH and DPO, in both phases, a single peak was observed for carbons C(2),C(2′) and C(3),C(3′) of the phenyl group. This was initially interpreted as due to a limited influence of the side chain conformation on the chemical shifts of

the carbons on the phenyls. However, as it will be shown below, QM computations indicate that it should be ascribed instead to a fast internal rotation. Analogous effects were observed also by Pines and co-workers [38] in their first ^{13}C-NMR studies of nematic liquid crystals. In addition, for DPO, the lines corresponding to carbons C(7) and C(8) are overlapped both in the in isotropic phase and in the whole nematic range.

2.2 Quantum mechanical computations

All calculations have been performed using a locally modified version of the Gaussian03 package.[39] Prior to computing the nuclear magnetic tensor, all molecular structures were optimized for isolated molecules, using PBE0 functional[40] (vide infra) and 6-31G+(d,p) basis set.[41–43] Two local minima have been investigated for each polyene, corresponding to *all-s-trans* and *all-s-cis* conformers, in order to evaluate how the flexibility of the olephinic chain may affect the magnetic behavior of ^{13}C nuclei. For all diphenylpolyenes the *all-s-trans* rotamers are more stable than the *all-s-cis* corresponding conformers: at 298.15 K enthalpy differences of 3.6, 7.0 and 10.8 kcal/mol have been computed for DPB, DPH and DPO, respectively. Results from fluorescence experiments provide extrapolated enthalpy differences for DPB equal to 1.9 ± 0.1 kcal/mol in methylcyclohexane and 2.3 ± 0.3 in toluene, pointing out the high solvent dependence for such measurements.[44] Analogous results for DPH lead to an estimated ΔH of 2.9 kcal/mol for each σ bond *in vacuum*.[45] Moreover, DFT calculations on DPH suggest $\Delta H = 3.4$ kcal/mol for each σ bond.[45] Experimental findings for 1,3-butadiene and parent molecules suggest that the introduction of each *s-cis* moiety should raise the energy by about 3 kcal/mol.[46,47]

DPE, DPB, DPH and DPO have a planar (C_{2h}) structure, while BP has a twisted (D_2) geometry with a twist angle of 38.8°, in good agreement with the experimental value in solution ($34 \pm 1°$).[48] Trans-stilbene is known to have an high torsional flexibility,[49] regarding the rotation of the phenyl groups. The computed rotational barriers for all *s-trans* polyenes are 4.5, 5.0, 5.3 and 5.4 kcal/mol for DPE, DPB, DPH and DPO, respectively. Calculations performed at PBE0/6-31+G(d,p) level are in excellent agreement with a comprehensive computational study of trans-stilbene in

Ref.49. Energy barriers of 4-5 kcal/mol are sufficiently low to be easily overtaken at the temperatures of the present experiments and in the time scale of NMR technique: the magnetically equivalent carbons in the phenyl moiety, nominally C(2),C(2') and C(3),C(3') thus cannot be distinguished due to the fast torsional motion.

The nuclear magnetic tensors have been calculated using the GIAO (gauge-independent atomic orbitals) method[50] and the PBE0[40] hybrid density functional based on the Perdew, Burke, and Ernzerhof[51] correlation and exchange functionals. As in all hybrid functionals, the exchange part is corrected by a prefixed amount of Hartree-Fock (nonlocal) exchange.[52] In particular, PBE0 provides accurate magnetic parameters for a large number of organic molecules.[14,18] In previous works,[18,20] we tested the Pople family of basis sets 6-31G,[41] with different contraction schemes and the addition of polarization[43] and diffuse functions:[42] the best compromise between accuracy and computational demand was obtained by the 6-311+G(2d,p) basis set, which was therefore used in all the following calculations.

The α,ω-diphenylpolyenes dissolved in liquid crystals feel an anisotropic environment which can be reproduced using the polarizable continuum model (PCM).[17,53] In PCM the solute molecule (or a small cluster including few solvent molecules, when needed[54]) is hosted in a cavity of suitable shape[55] within the solvent, represented as an infinite dielectric medium and characterized by the dielectric constant. The solvent reaction field is expressed in terms of a set of apparent charges spread on the cavity walls. The model has also been extended to anisotropic solvents,[19,53] for which a dielectric tensor has to be defined instead of a simple dielectric constant. Recently, the anisotropic version of PCM has been reformulated so that the solvation charges are computed in terms of the solute electrostatic potential, with the same formal expression used for isotropic solvents.[53c] PCM is particularly suitable for the calculation of magnetic parameters,[56] because its most recent implementations require computational resources comparable to those needed for isolated molecules. For the present computations we adopted $\epsilon_{||} = 8.1$, $\epsilon_{\perp} = 4.0$ (data for ZLI-1167 at T = 336 K[29]) with $\epsilon_{||}$ and the C(1)-H bond of each structure aligned with the Z axis (nematic director). Variations of the dielectric anisotropy within the temperature range of the experiment

were neglected.

2.3 Data analysis

The molecules studied here have, in their energetically most stable configuration, a relatively high symmetry (D_2 for BP, C_{2h} for the *s-trans* diphenylpolyenes, C_{2v} for the *s-cis* diphenylpolyenes). However, such an high symmetry can be safely assumed only for BP and DPE, since DPB, DPH and DPO backbone flexibility allows a fast interconversion between *s-trans* and *s-cis* forms.[44–47] In addition, internal rotations of the phenyl rings are always possible, except for BP.

In the present experiment, for each chemically different nucleus J, the observables are the temperature dependent differences between $\sigma_J^{\rm aniso}$ and $\sigma_J^{\rm iso}$, the carbon chemical shifts in the ordered and in the isotropic phases, respectively. These are related to the orientational average of the component of the shielding tensor σ parallel to the laboratory Z-axis (or, equivalently, the (2,0) component using spherical tensors), fixed by the magnetic field direction (see e.g. Ref.5).

$$\sigma_J^{\rm aniso} - \sigma_J^{\rm iso} = \left\langle \sigma_{J;ZZ}^{\rm LAB} \right\rangle_{\omega;\phi} = \sqrt{\tfrac{2}{3}} \left\langle \sigma_{J;{\rm LAB}}^{2,0} \right\rangle_{\omega;\phi}. \tag{1}$$

The average $\langle \cdots \rangle_{\omega;\phi}$ is meant to be extended either to the orientation ω of the molecule in the laboratory frame, if it can be treated as a rigid object (see. e.g. Ref.2) or, in the case of non-rigid solutes, to the orientation ω of a reference fragment as well as to the relative orientations $\phi_1, \phi_2, ...$ of all rigid sub-units with respect to the reference one. [57] In the most general case, the $\langle \sigma_{J;{\rm LAB}}^{2,0} \rangle_{\omega;\phi}$ experimental observables should be written as:

$$\left\langle \sigma_{J;{\rm LAB}}^{2,0} \right\rangle_{\omega;\phi} \equiv \int \sigma_{J;{\rm LAB}}^{2,0}(\omega;\phi) P(\omega;\phi)\, d\omega\, d\phi \tag{2}$$

where ω is the orientation of a rigid reference fragment, ϕ denotes collectively the set of angles $\phi_1, \phi_2, ..., \phi_n$ required to uniquely specify the orientation of any rigid subunit of the molecule with respect to the reference fragment, and $P(\omega;\phi)$ is the probability of finding the molecule at the orientation $\{\omega;\phi\}$

If the director of the mesophase does not coincide with the laboratory Z axis, a first rotation is needed to change the frame:

$$\left\langle \sigma^{2,0}_{J;\mathrm{LAB}}(\omega;\phi)\right\rangle_{\omega;\phi} = P_2(\mathrm{DIR}\rightarrow\mathrm{LAB})\left\langle \sigma^{2,0}_{J;\mathrm{DIR}}(\omega;\phi)\right\rangle_{\omega;\phi} \tag{3}$$

Assuming uniaxial symmetry for the liquid crystal around the director, this rotation is described by a simple multiplicative factor ($<\sigma_J^{LAB}>= S_f <\sigma_J^{DIR}>$): for ZLI-1167 the director aligns perpendicularly to the external magnetic field and $S_f = \langle P_2(\mathbf{d}\cdot\mathbf{B})\rangle = -0.5$.

A further rotation from the director frame to a molecular (local) frame embedded on the reference fragment leads to:

$$\begin{aligned}\left\langle \sigma^{2,0}_{J;\mathrm{DIR}}(\omega;\phi)\right\rangle_{\omega;\phi} &= \sum_n \left\langle D^{2*}_{0,n}(\mathrm{MOL}\rightarrow\mathrm{DIR})\sigma^{2,0}_{J;\mathrm{MOL}}(\omega;\phi)\right\rangle_{\omega;\phi} \\ &= \sum_n \int D^{2*}_{0,n}(\omega)\sigma^{2,n}_{J;\mathrm{MOL}}(\omega;\phi)P(\omega;\phi)\,d\omega\,d\phi \end{aligned} \tag{4}$$

Workable expressions can be obtained only by making some assumptions:

i) $P(\omega;\phi)$ is factorisable into $P_\omega(\omega)P_\phi(\phi)$, equivalent to say that the internal conformation does not affect the overall molecular order. This is in general quite a strong assumption, but in the present case it can be safely invoked since the rotational isomerism around σ bonds does not radically change the elongated rod-like shape of the molecules. A corollary assumption, needed to make the analysis feasible, is that the conformational distribution $P_\phi(\phi)$ is essentially temperature independent.

ii) Changes in $\sigma^{2,0}_{J;\mathrm{MOL}}(\omega;\phi)$ due to the orientation ω of the molecule in the anisotropic medium are negligible. This assumption was implicitly taken in all our previous works, [26–28] and some recent studies [20,58] have confirmed its applicability. In calculating the shielding tensors, we then keep the molecule aligned with the cylindrical axis of the dielectric tensor and we assume that the values of the tensor components do not significantly depend on the molecular orientation.

Under the above assumptions, eq.4 can be rewritten as:

$$\left\langle \sigma^{2,0}_{J;\mathrm{DIR}}(\omega;\phi)\right\rangle_{\omega;\phi} = \sum_n \int D^{2*}_{0,n}(\omega)P_\omega(\omega)d\omega \cdot \int \sigma^{2,n}_{J;\mathrm{MOL}}(\phi)P_\phi(\phi)\,d\phi$$

$$= \sum_n \left\langle D^{2*}_{0,n} \right\rangle \left\langle \sigma^{2,n}_{J;\mathrm{MOL}} \right\rangle_\phi \tag{5}$$

By combining eqs.1-5, and taking advantage of the symmetry relation $\langle D^{2*}_{0n} \rangle = (-1)^n \langle D^2_{0-n} \rangle$, we obtain

$$\begin{aligned} \sqrt{\frac{3}{2}} \frac{\sigma_J^{\mathrm{aniso}} - \sigma_J^{\mathrm{iso}}}{P_2(\mathrm{DIR} \to \mathrm{LAB})} &= \left\langle D^2_{00} \right\rangle \left\langle \sigma^{2,0}_{J;\mathrm{MOL}} \right\rangle_\phi \\ &+ \left\langle D^2_{01} \right\rangle \left(\left\langle \sigma^{2,1}_{J;\mathrm{MOL}} \right\rangle_\phi - \left\langle \sigma^{2,-1}_{J;\mathrm{MOL}} \right\rangle_\phi \right) \\ &+ \left\langle D^2_{02} \right\rangle \left(\left\langle \sigma^{2,2}_{J;\mathrm{MOL}} \right\rangle_\phi + \left\langle \sigma^{2,-2}_{J;\mathrm{MOL}} \right\rangle_\phi \right) \end{aligned} \tag{6}$$

which can be rewritten in terms of Cartesian instead of spherical tensor components:

$$\begin{aligned} \sqrt{\frac{3}{2}} \frac{\sigma_J^{\mathrm{aniso}} - \sigma_J^{\mathrm{iso}}}{P_2(\mathrm{DIR} \to \mathrm{LAB})} &= \sqrt{\tfrac{3}{2}} \left\langle D^2_{00} \right\rangle \left\langle \sigma^{\mathrm{MOL}}_{J;ZZ} \right\rangle_\phi \\ &- \left\langle D^2_{01} \right\rangle \left(\left\langle \sigma^{\mathrm{MOL}}_{J;XZ} \right\rangle_\phi + \left\langle \sigma^{\mathrm{MOL}}_{J;ZX} \right\rangle_\phi \right) \\ &+ \left\langle D^2_{02} \right\rangle \left(\left\langle \sigma^{\mathrm{MOL}}_{J;XX} \right\rangle_\phi - \left\langle \sigma^{\mathrm{MOL}}_{J;YY} \right\rangle_\phi \right) \end{aligned} \tag{7}$$

The local fragment frame, embedded on the phenyl rings of each structure and taken as molecular frame, is depicted in figure 7. The phenyl ring behaves, with respect to the present experimental resolution, as an effective D_{2h} object. In fact, reflection about YZ plane converts carbons C(2) into C(2′) and C(3) into C(3′), which are experimentally indistinguishable due to fast rotation, while a "pseudo-reflection" (reflection+translation) about the XY plane overlaps the fragment onto the other phenyl. Such effective D_{2h} symmetry makes identically null the $\langle D^2_{01} \rangle$ order parameter in eq.(6-7), hence the only non-zero order parameters are $\langle D^2_{00} \rangle \equiv \langle P_2 \rangle$ and $\langle D^2_{02} \rangle$. Under the above assumptions, data analysis can then be set up in the same way as for rigid molecules; however, the recovered data assume a slightly different physical meaning.

The effects of internal conformation ϕ on the shielding tensors may obviously be somewhat different, depending on the carbon which is considered. C(1),C(4) are reasonably unaffected, for C(2),C(2′) the dependence is small, while for C(3),C(3′) it is very large (see next section). For C(5)-C(8) the effects may depend both on the chain length and on its conformation.

The thermally activated rotation of the phenyl group leads to a simple switch model for evaluating $P_\phi(\phi)$, considering only two (magnetically equivalent) conformations of the phenyl group irrespective of the conformation of the chain. In practice the effective values for the tensor components of carbons C(2),C(2′) and C(3),C(3′), needed to perform the analysis of the experimental data, are taken to be the arithmetic mean of the theoretically calculated values.

Similarly, the shielding tensor components retrieved from the analysis should be considered as effective average values.

Experimental data were analyzed using eq.(7) and two different methods:
(a) taking as reference carbons C(1),C(2) and using benzene solid state shielding tensor [59] or
(b) taking as reference carbons C(1),C(2),C(3),C(4) and using ab initio shielding tensors, both for the *s-trans* and *s-cis* forms, with averaged tensor components for carbons C(2) and C(3).

3 Results and Discussion

3.1 Carbon shieldings

In Table 1 we summarize the computed results for the shielding tensors of BP, DPE and both *s-cis* and *s-trans* rotamers of DPB, DPH and DPO. For each chemically different carbon we report the chemical shift σ_{iso} (the trace of the shielding tensor), referred to chemical shift of carbon C(1) of each structure, $\sigma_{11}, \sigma_{22}, \sigma_{33}$, the tensor principal components, and γ, the in-plane orientation of the least shielded principal axis of the tensor, again referred to the C(1) principal frame. This choice permits an easier comparison of the results for corresponding carbons in different structures, and a more effective comparison with the experimental data. In Fig. 8, experimental and calculated (*s-trans* structures) isotropic relative chemical shifts, are compared.

It is evident that for DPE, DPB, DPH and DPO, the carbons C(3),C(3′) have a difference of ≈8 p.p.m. in the calculated isotropic chemical shift, while for carbons C(2),C(2′), the difference is ≈1 p.p.m.. This is at odds with the experimental findings,

both in the isotropic phase and in the nematic phase, were a single signal originates from these couples of carbons. The fact that, experimentally, a single signal is always observed, in a position about halfway between the theoretical predictions, is an evidence that, at the temperatures of the experiment, the phenyl groups have a high rotational mobility with respect to the polyenic chain.

The differences, in the isotropic shift of the DPB, DPH and DPO *s-trans* and *s-cis* conformers, are rather limited for the aromatic carbons, while they are quite large (> 5 p.p.m.) for the polyenic chain carbons.

The observed chemical shifts for olefinic carbons are better reproduced by the calculated *s-trans* shifts, indicating that, at least in the isotropic phase, this form is strongly dominant.

A valuable indication of the consistency of the data analysis can be inferred on inspection of the recovered shielding tensors of the carbons not taken as reference, i.e. C(3)-C(8). Those recovered from method (a) are collected in Table 2. Our experimental approach is not able to recover the principal frame orientation, hence only fragment frame cartesian components are reported and compared to DFT values.

In the systems under study we have three types of carbons: protonated aromatic C(1)–C(3), quaternary aromatic C(4) and olefinic C(5)–C(8).

Except for BP, the recovered tensors for C(3) and C(4) are close to their DFT counterparts, and these in turn are very close to the typical values of protonated and quaternary aromatic carbons, respectively ($\sigma^{\mathrm{MOL}}_{C(3);XX} = 82, \sigma^{\mathrm{MOL}}_{C(3);YY} = -120, \sigma^{\mathrm{MOL}}_{C(3);ZZ} =$ 38 p.p.m [59,60] and $\sigma^{\mathrm{MOL}}_{C(4);XX} = 29, \sigma^{\mathrm{MOL}}_{C(4);YY} = -127, \sigma^{\mathrm{MOL}}_{C(4);ZZ} = 99$ p.p.m [61]) proving that the assumptions made for the reference carbons are fully consistent.

For BP the recovered C(3),C(4) tensor components are, on the other hand, fairly different from DFT values, but closer to experimental solid state values ($\sigma^{\mathrm{MOL}}_{C(3);XX} =$ $68, \sigma^{\mathrm{MOL}}_{C(3);YY} = -102, \sigma^{\mathrm{MOL}}_{C(3);ZZ} = 34$ p.p.m, $\sigma^{\mathrm{MOL}}_{C(4);XX} = 20, \sigma^{\mathrm{MOL}}_{C(4);YY} = -114, \sigma^{\mathrm{MOL}}_{C(4);ZZ} =$ 94 p.p.m [37,60]). This may be interpreted, as in Ref. 37 in terms of an effect of librations around the phenyl-phenyl bond. In this respect, BP is unique among the molecules considered in this study, since phenyl rotations can not be assumed as uncorrelated: as a matter of fact a rotation of a phenyl along the ring linkage averages the effective

tensors due to opposing changes in tensor orientations.

Tensor components of olefinic carbons C(5)–C(8) are much more difficult to rationalize. The experimental information about this type of carbons is more limited,[62] especially for highly conjugated chains. [63,64]

Bearing in mind that the present analysis is able to recover just averaged effective values for these carbons, under the assumptions quoted in section 2.3, we can try to infer some information about chain conformations by comparing the experimentally recovered values to their DFT counterparts, corresponding either to full *s-trans* or to full *s-cis* conformations.

Experimentally, we observed some apparent trends for the tensor components of carbons occupying the same positions in different chains. For example, the $\sigma^{MOL}_{C(5);XX}$ component increases steadily from DPE to DPO while the opposite trend is observed for $\sigma^{MOL}_{C(5);YY}$ and $\sigma^{MOL}_{C(5);ZZ}$. Similar trends are observed for C(6) and C(7).

These trends, however, are not reproduced by the DFT computations, neither by the *s-trans*, nor by the *s-cis* forms: indeed, for corresponding carbons, the shielding tensors are predicted to remain essentially constant with chain length. In practice, for olefinic carbons, a reasonably good match between guess values in the iterative procedure issuing from theory and experiment is obtained only for the shortest member of the series, i.e. for DPE. In this case we obtained also a very good agreement between our experimental values and a literature value derived from solid state experiments ($\sigma^{\mathrm{MOL}}_{C(5);XX} = 35, \sigma^{\mathrm{MOL}}_{C(5);YY} = -79, \sigma^{\mathrm{MOL}}_{C(5);ZZ} = 43$ p.p.m [65,66])

In summary, the spacer chain conformations does not seem to be responsible for the observed trends in DPB,DPH and DPO and the molecular origin of such effects remains an open question.

Moreover, it is known that DFT methods may lack in accuracy in the calculation of some properties (e.g. polarizabilities or UV transitions)[67,68] for highly conjugated systems: since to the best of our knowledge, nothing has been reported about chemical shielding tensors, a further investigation is needed. Anyway, as only the shielding of the aromatic carbons are needed for the calculation of the order parameters, this shortcoming is not affecting the final results presented here and the DFT approach is

trustworthy for such systems.

3.2 Order parameters

The second rank order parameters obtained from methods (a) and (b) employing the two different choices of reference carbons are summarized in Fig. 9. The two sets of results are very similar, again indicating that the use of benzene shielding tensors for carbons C(1) and C(2) is a good approximation. The trend of the biaxial $\langle D^2_{02} \rangle$ vs. uniaxial $\langle P_2 \rangle$ order is similar for the various solutes studied and follows the classical trend, studied long time ago with molecular field theory.[69] In the same figure we also show our estimate for the error bounds on the recovered order parameters. As in our previous paper [20], to estimate the errors we have randomly varied the shielding tensors of the reference carbons within 3 ppm for the tensor components and within 2° for the in-plane principal axis orientation, keeping track of the effects on the recovered order parameters.

Even though our study is focused on the determination of the order parameters in the polyene series, rather than in discussing their molecular origin, we wish to provide at least an indication of the effect of molecular size and a comparison with a few data available for our solute-solvent system from other techniques. In Fig. 10 we compare the order parameters, as a function of the spacer length, at three reduced temperatures sampling the whole nematic range. We can see that $\langle P_2 \rangle$ increases steadily with the length of the molecule, at any temperature within the nematic range, while $\langle D^2_{02} \rangle$ is always small and essentially constant, with a slight tendency to decrease with length. This finding gives further support to the common practice in spectroscopic studies [31] of assuming diphenyl-polyenes as having an effective uniaxial symmetry.

It is also interesting to compare the order parameters, obtained for DPH [29] and DPO [30] in the same liquid crystal solvent with fluorescence depolarization technique, to those obtained in the present work. We see from Fig. 10 that the order parameters obtained for DPH from fluorescence and NMR are very close, while for DPO the order parameters obtained from fluorescence show a larger dependence from temperature.

4 Conclusions

In the present work, we have applied a combined computational and experimental approach to evaluate the order parameters of a set of molecules dissolved in liquid crystals. We studied the orientational behavior of a series of α,ω-diphenylpolyenes, which are often used as molecular probes in fluorescence polarization experiments. Even if they show a high structural flexibility due to rotamerism and to torsional freedom of the phenyl group, a cylindrical effective symmetry has proven to be a reliable approximation.

Order parameters of these molecules are obtained from temperature dependent, natural abundance, ^{13}C NMR measurements and from quantum mechanical calculations of carbon shielding tensors. The data analysis model proves to recover order parameters of quality comparable to deuterium NMR-based methods, with the advantage of bypassing all complications arising from the synthesis of deuterated molecules. Modern quantum mechanical techniques, taking into account anisotropic solvent effects, provide a realistic description of the environment surrounding the probe and therefore lead to accurate values of the shielding tensors.

The present work shows that our approach can be usefully applied to classes of relatively large molecules of great importance for their use as probes of molecular organization in a variety of oriented fluids, allowing for solute molecular conformational freedom. There are of course continuous progresses in other ^{13}C NMR spectroscopical techniques, e.g. in determining H-^{13}C dipolar couplings via 2D NMR spectroscopies[10,11]. Some of these approaches have been recently used to determine the order of bulk complex mesogens [70]. However, we believe that it would be very difficult to obtain the type of detailed orientational information presented here on solutes in rather low concentration with other techniques and we trust that the present data will provide a useful test-bed for molecular theories of solute ordering in liquid crystals.

5 Acknowledgments

We are grateful to MIUR (COFIN "Modelling and characterization of liquid crystals for nano-organized structures") and INSTM (PRISMA project) for support. We are also particularly indebted to Mr. D. Macciantelli (ISOF, CNR) and to Dr. D. Casarini for their help in running the experiments and to Prof. L. Lunazzi for the use of the CXP300 spectrometer. All the calculations have been performed using the advanced computing facilities of the "Campus Grid" - University Federico II, Naples.

References

[1] D.A. Dunmur, A. Fukuda, and G.R. Luckhurst, *Physical Properties of Liquid Crystals: Nematics* (IEE, London, 2001).

[2] C. Zannoni in *Nuclear Magnetic Resonance of Liquid Crystals*, edited by J. W. Emsley (Reidel, Dordrecht, 1985), ch. 1, p. 1.

[3] E. E. Burnell and C. A. de Lange, Chem. Rev. **98**, 2359 (1998).

[4] B. Bahadur, *Liquid Crystals Applications and Uses* (Word Scientific, Singapore, 1991).

[5] J. W. Emsley, editor, *Nuclear Magnetic Resonance of Liquid Crystals*, (Reidel, Dordrecht, 1985).

[6] T. Nakai, H. Fujimori, D. Kuwahara, and S. Miyajima, J. Phys. Chem. B **103**, 417 (1999).

[7] J. Xu, K. Fodor-Csorba, and R. Y. Dong J. Phys. Chem. A **109**, 1998 (2005).

[8] R.Y. Dong, K. Fodor-Csorba, J. Xu, V. Domenici, G. Prampolini, and C.A. Veracini, J. Phys. Chem. B **108**, 7694 (2004).

[9] Z. Huang, D. Sandström, U. Henriksson, and A. Maliniak, J. Phys. Chem. B **102**, 8395 (1998).

[10] B.M. Fung, Prog. Nucl. Magn. Reson. Spectrosc. **41**, 171 (2002).

[11] R.Y. Dong, *Annu. Rep. NMR Spectrosc.* **53**, 67 (2004).

[12] T. Helgaker, M. Jaszunski, and K. Ruud, Chem. Rev. **99** 293 (1999).

[13] T.H. Sefzik, D. Turco, R.J. Iuliucci, J.C. Facelli, J. Phys. Chem. A **109**, 1180 (2005).

[14] (a) C. Adamo, M. Cossi, N. Rega, and V. Barone, in Theoretical Biochemistry. Processes and Properties of Biological Systems, edited by L. Erikkson (Elsevier,2001), p. 467. (b) V. Barone, O. Crescenzi, and R. Improta, Quant. Struct. Act. Relat. **21**, 105 (2002).

[15] R. Improta, and V. Barone, Chem. Rev. **104**, 1231 (2004).

[16] W. Koch and M.C. Holthausen, in *A Chemist's Guide to Density Functional Theory* (Wiley-VCH, Weinheim, 2000).

[17] (a) S.Miertus, E. Scrocco, and J. Tomasi, J. Chem. Phys. **55**, 117 (1981); (b) M. Cossi, G. Scalmani, N. Rega, and V. Barone, J. Chem. Phys. **117**, 43 (2002).

[18] C. Benzi, O. Crescenzi, M. Pavone, and V. Barone, Magn. Reson. Chem. **42**, S57 (2004).

[19] C. Benzi, M. Cossi, and V. Barone, J. Chem. Phys. **123**, 194909 (2005).

[20] C. Benzi, M. Cossi, V. Barone, R. Tarroni, and C. Zannoni, J. Phys. Chem. B. **109**, 2584 (2005).

[21] M. Strohmeier, and D.M. Grant, J. Am. Chem. Soc. **126**, 966 (2004).

[22] D.H. Barich, R.J. Pugmuire, D.M. Grant, and R.J. Iuliucci, *J. Phys. Chem. A* **105**, 6780 (2001).

[23] A. M. Orendt, Magn. Res. Chem. **44**, 385 (2006).

[24] R. Eidenschink, D. Erdmann, J. Krause, and L. Pohl, Angew. Chem. Int. Ed. Engl. **17**, 133 (1978).

[25] H. Wedel and W. Haase, Chem. Phys. Lett. **55**, 96 (1978).

[26] A. Hagemeyer, R. Tarroni, and C. Zannoni, J. Chem. Soc. Faraday Transactions **90**, 3433 (1994).

[27] R. Tarroni, and C. Zannoni, J. Phys. Chem. **100**, 17157 (1996).

[28] R. Tarroni, and C. Zannoni, Chem. Phys. **211**, 337 (1996).

[29] A. Arcioni, F. Bertinelli, R. Tarroni, and C. Zannoni, Mol. Phys. **61**, 1161 (1987).

[30] A. Arcioni, F. Bertinelli, R. Tarroni, and C. Zannoni, Chem. Phys. **143**, 259 (1990).

[31] B. R. Lenz, Chem. Phys. Lipids **64**, 99 (1993).

[32] M. Allen, and D. Whitten, Chem. Rev. **89**, 1961 (1989).

[33] J. Repakova, P. Capkova, J.M. Holopainen, and I. Vattulainen, J. Phys. Chem. B **108**, 13438 (2004).

[34] A. Kintanar, A.C. Kunvar, and E. Oldfield, Biochemistry **25**, 6517 (1986).

[35] E.M. Schulman, K.A. Christensen, D.M. Grant, and C. Walling, J. Org. Chem. **39**, 2686 (1974).

[36] L.M. Tolbert, and M.E. Ogle, J. Am. Chem. Soc. **112**, 9519 (1990).

[37] D.H. Barich, R.J. Pugmire, D.M. Grant, and R.J. Iuliucci, J. Phys. Chem. A **105**, 6780 (2001).

[38] A. Pines, D.J. Ruben, and S. Allison, Phys. Rev. Lett. **33**, 1002 (1974).

[39] M. J. Frisch *et al.*, Gaussian 03, Revision C.04 (Gaussian Inc., Pittsburgh PA, 2003)

[40] C. Adamo, and V. Barone, J. Chem. Phys. **110**, 6158 (1999).

[41] M.J. Frisch, J.A. Pople, and J.S. Binkley, J. S., J. Chem. Phys. **80**, 3265 (1984).

[42] G.A. Petersson and M.A. Al-Laham, J. Chem. Phys. **94**, 6081 (1991).

[43] T.H. Dunning, Jr., J. Chem. Phys. **90**, 1007 (1989).

[44] C.E. Bunker, C.A. Lytle, H.W. Rollins, and Y.-P. Sun, J. Phys. Chem. A **101**, 3214 (1997).

[45] A.M. Turek, G. Krishnamoorthy, D.F. Sears, Jr., I. Garcia, O. Dmitrenko, and J. Saltiel, J. Phys. Chem. A **109**, 293 (2005).

[46] J. Saltiel, D.F Sears, Y.-P. Sun, and J.-O. Choi, J. Am. Chem. Soc. **114**, 3607 (1992).

[47] Y. -P. Sun, C.E. Bunker, P.L. Wickremesinghe, H.W. Rollins, and G.E. Lawson J. Phys. Chem. **99**, 3423 (1995).

[48] G. Celebre, G. De Luca, M. Longeri, D. Catalano, C.A. Veracini, and J.W. Emsley, J. Chem. Soc. Faraday Trans. **87**, 2623 (1991).

[49] S. P. Kwasniewski, L. Claes, J.-P. François, and M.S. Deleuze, J. Chem. Phys. **118**, 7823 (2003).

[50] K. Wolinski, J. F. Hilton, and P. Pulay, J. Am. Chem. Soc. **112**, 8251 (1990).

[51] J. P. Perdew, M. Ernzerhof, and K. Burke, J. Chem. Phys. **105**, 9982 (1996).

[52] A.D. Becke, J. Chem. Phys. **104**, 1040 (1996).

[53] (a) B. Mennucci, E. Cancès, and J. Tomasi, J. Phys. Chem. B **101**, 10506 (1997); (b) E. Cancès and B. Mennucci J. Math. Chem. **23**, 309 (1998); (c) B. Mennucci and R. Cammi Int. J. Quant. Chem. **93**, 121 (2003).

[54] (a) M. Pavone, C. Benzi, F. Angelis, and V. Barone, Chem. Phys. Lett. **395**, 120 (2004); (b) R. Improta and V. Barone, J. Am. Chem. Soc. **126**, 14320 (2004).

[55] (a) J.-L. Pascual-Ahuir, E. Silla, and I. Tuñon, J. Comput. Chem. **15**, 1127 (1994); (b) G. Scalmani, N. Rega, M. Cossi, and V. Barone, J. Comput. Meth. Sci. Eng. **2**, 469 (2002).

[56] R. Cammi, B. Mennucci, and J. Tomasi, J. Chem. Phys. **110**, 7627 (1999).

[57] C. Zannoni, in *Nuclear Magnetic Resonance of Liquid Crystals*, edited by J. W. Emsley (Reidel, Dordrecht, 1985), ch. 2, p. 35.

[58] M. Pavanello, B. Mennucci, and A. Ferrarini, J. Chem. Phys. **122**, 064906 (2005).

[59] H. Strub, A.J. Beeler, D.M. Grant, J. Michl, P.W. Cutts, and K.W. Zilm, J. Am. Chem. Soc. **105**, 3333 (1983).

[60] These molecular values have been derived from the principal values reported in Refs.[37, 59, 61] assuming the molecular frame of fig.7 and an in-plane rotation of 60° for C(3) principal frame

[61] J. van Dongen Torman and W.S. Veeman, J. Chem. Phys. **68**, 3233 (1978).

[62] A.M. Orendt, J.C. Facelli, A.J. Beeler, K. Reuter, J.W. Horton, P. Cutts, D.M. Grant, and J. Michl, J. Am. Chem. Soc. **110**, 3386 (1988).

[63] T. Duncan, J. Phys. Chem. Ref. Data **16**, 125 (1987).

[64] T. Nakay, T. Terao, and H. Shirakawa, Chem. Phys. Lett. **145**, 90 (1988).

[65] G. M. Bernard, G. Wu, and R. E. Wasylishen, J. Phys. Chem. A **102**, 3184 (1998).

[66] These molecular values for C(5) of DPE have been derived from the principal values reported in Ref.65, assuming the molecular frame of fig.8 and an in-plane rotation of 42.9°, as deduced from Table 1

[67] R. Spezia, C. Zazza, A. Palma, A. Amadei, and M. Aschi, J. Phys. Chem. A **108**, 6763 (2004).

[68] B. Champagne, E.A. Perpete, D. Jacquemin, S.J.A. Van Gisbergen, E.J-. Baerends, C. Soubra-Ghaoui, K.A. Robins, and B. Kirtman, J. Phys. Chem. A **104**, 4755 (2000).

[69] G.R. Luckhurst, C. Zannoni, P.L. Nordio, and U. Segre, Mol. Phys. **30**, 1345 (1975).

[70] J. Xu, K. Fodor-Csorba and R. Y. Dong, J. Phys. Chem. A 109, 1998 (2005).

[71] Order parameters at the three reduced temperatures $T* = 0.99, 0.93, 0.88$ are obtained from the empirical function $\langle P_2 \rangle(T) = 0.7821(1 - T/355)^{0.1679}$, which in turn is obtained from a fitting of the experimental data of Ref.29

[72] Order parameters at the three reduced temperatures $T* = 0.99, 0.93, 0.88$ are obtained from the empirical function $\langle P_2 \rangle(T) = 1.0123(1 - T/355)^{0.1922}$, which in turn is obtained from a fitting of the experimental data of Ref.30

Table 1: Calculated carbon isotropic shifts and shielding tensors principal values (p.p.m.) for biphenyl (BP), trans-stilbene (DPE), 1,4-diphenyl-butadiene (DPB), 1,6-diphenyl-hexatriene (DPH), and 1,8-diphenyl-octatetraene (DPO), in an anisotropic solvent with $\epsilon_{||} = 8.1, \epsilon_{\perp} = 4.0$, with $\epsilon_{||}$ oriented along the Z axis . γ (degrees) is defined in section 3.1

carbon	shielding tensor	BP	DPE	DPB		DPH		DPO	
				s-trans	s-cis	s-trans	s-cis	s-trans	s-cis
	σ_{iso}	0.0	0.0	0.0	0.0	0.0	0.0	0.0	0.0
1	σ_{11}	111.7	109.4	108.9	109.2	108.7	109.2	108.5	109.1
	σ_{22}	12.9	14.5	14.8	14.3	14.9	14.5	14.7	14.4
	σ_{33}	-124.6	-123.9	-123.7	-123.9	-123.6	-123.7	-123.3	-123.4
	γ	0.0	0.0	0.0	0.0	0.0	0.0	0.0	0.0
	σ_{iso}	-1.5	-0.6	-0.9	-0.7	-1.0	-0.8	-0.8	-0.8
2	σ_{11}	110.8	111.8	111.8	111.7	112.0	111.8	112.0	111.9
	σ_{22}	13.6	12.8	12.8	13.2	12.7	13.0	12.8	13.1
	σ_{33}	-124.5	-124.6	-124.5	-124.9	-124.7	-124.8	-124.8	-125.0
	γ	60.1	61.3	61.2	61.2	61.3	61.3	61.3	61.4
	σ_{iso}		-1.5	-1.5	-1.0	-1.7	-1.1	-1.5	-1.1
$2'$	σ_{11}		112.0	111.5	111.2	111.3	111.8	111.2	111.4
	σ_{22}		12.4	12.3	12.6	12.1	12.7	12.1	12.5
	σ_{33}		-124.3	-123.8	-123.9	-123.4	-124.5	-123.3	-123.9
	γ		-59.0	-59.3	-58.9	-59.5	-59.1	-59.4	-59.0
	σ_{iso}	-0.6	5.2	5.1	5.8	5.2	5.0	5.6	5.7
3	σ_{11}	102.9	105.4	104.0	104.9	104.4	104.5	104.4	104.8
	σ_{22}	13.0	16.9	18.0	17.6	18.6	16.8	18.5	17.8
	σ_{33}	-115.9	-122.3	-122.1	-122.5	-123.0	-121.3	-122.8	-122.6
	γ	-65.3	-62.0	-63.1	-62.7	-63.8	-62.5	-63.5	-62.9
	σ_{iso}		-2.9	-3.0	-2.7	-3.1	-2.9	-3.2	-2.9
$3'$	σ_{11}		99.9	99.0	99.4	99.0	99.5	99.0	99.3
	σ_{22}		10.5	11.4	10.7	11.3	11.0	11.3	10.8
	σ_{33}		-110.4	-110.5	-110.1	-110.3	-110.4	-110.3	-110.2
	γ		63.0	63.0	63.2	63.0	63.5	63.1	63.4
	σ_{iso}	-16.0	-9.8	-9.3	-9.2	-9.3	-9.5	-9.4	-9.5
4	σ_{11}	93.1	94.1	93.4	93.2	93.2	92.6	92.7	92.4
	σ_{22}	36.1	37.7	36.8	38.2	37.4	39.3	37.7	39.3
	σ_{33}	-129.1	-131.8	-130.2	-131.5	-130.6	-131.9	-130.4	-131.7
	γ	0.0	0.7	0.4	-0.6	0.5	-0.9	-0.5	-0.8
	σ_{iso}		-0.8	-6.7	-1.3	-7.2	-1.7	-7.2	-1.5
5	σ_{11}		97.7	92.3	98.8	92.6	98.3	91.9	98.2
	σ_{22}		-7.4	-9.6	-6.0	-9.0	-4.9	-8.4	-5.0
	σ_{33}		-90.3	-82.7	-92.8	-83.5	-93.4	-83.5	-93.1
	γ		-42.9	-44.2	-42.5	-44.3	-43.1	-44.6	-42.9
	σ_{iso}			-2.3	6.5	-2.7	6.2	-1.9	5.0
6	σ_{11}			95.8	101.1	97.2	101.2	95.6	101.6
	σ_{22}			5.4	0.8	5.6	2.8	6.7	2.2
	σ_{33}			-101.2	-101.9	-102.7	-104.1	-102.3	-103.8
	γ			-47.8	-43.6	-48.8	-45.0	-49.1	-45.7
	σ_{iso}					-8.0	4.1	-8.5	3.9
7	σ_{11}					91.7	106.4	91.8	104.7
	σ_{22}					2.1	1.5	3.0	2.6
	σ_{33}					-93.9	-108.0	-94.8	-107.3
	γ					-50.4	-38.7	-50.7	-39.0
	σ_{iso}							-7.8	3.4
8	σ_{11}							91.8	105.4
	σ_{22}							3.1	2.7
	σ_{33}							-94.9	-108.1
	γ							-51.5	-39.8

Table 2: Comparison between the shielding components obtained from experiment and from ab initio calculations.

	shielding	BP		DPE		DPB			DPH			DPO		
carbon	tensor	exp.	calc.	exp.	calc.	exp.	calc.[c]	calc[d]	exp.	calc.[c]	calc[d]	exp.	calc.[c]	calc.[d]
3	XX	64.1	86.1	77.4	83.7[a]	72.9	83.8[a]	83.9[a]	77.7	84.3[a]	83.8[a]	77.3	84.2[a]	84.1[a]
	YY	-98.2	-114.7	-110.1	-116.4[a]	-106.3	-116.3[a]	-113.3[a]	-110.4	-116.7[a]	-115.9[a]	-110.1	-116.6[a]	-116.4[a]
	ZZ	34.1	28.6	32.7	32.7[a]	33.4	32.5[a]	32.4[a]	32.7	32.4[a]	32.0[a]	32.8	32.4[a]	32.23[a]
4	XX	9.7	34.6	27.6	37.7	33.1	36.8	38.2	36.7	37.4	39.3	34.6	37.7	39.3
	YY	-104.9	-127.7	-124.0	-131.8	-127.1	-130.2	-131.4	-131.4	-130.6	-131.9	-128.7	-130.4	-131.7
	ZZ	95.2	93.1	96.4	94.1	94.0	93.4	93.2	94.7	93.2	92.6	94.2	92.7	92.4
5	XX			35.1	41.3	60.4	40.0	42.0	77.8	40.5	43.3	95.8	41.0	42.8
	YY			-77.1	-90.3	-86.4	-82.7	-92.8	-96.7	-83.5	-93.4	-110.1	-83.5	-93.1
	ZZ			42.0	49.0	26.0	42.7	50.8	18.9	43.0	50.1	14.3	42.5	50.3
6	XX					66.6	55.0	48.6	77.9	57.5	52.1	93.2	57.5	53.1
	YY					-97.2	-101.1	-101.9	-103.2	-102.7	-104.1	-114.5	-102.3	-103.8
	ZZ					31.0	46.1	53.3	25.3	45.2	52.0	21.4	44.8	50.7
7	XX								95.1	55.4	42.5	108.2[b]	57.4	43.1
	YY								-112.8	-93.9	-108.0	-122.5[b]	-94.9	-107.3
	ZZ								17.7	38.5	65.5	14.3[b]	37.5	64.3
8	XX											108.2[b]	57.4	44.7
	YY											-122.5[b]	-94.9	-108.1
	ZZ											14.3[b]	37.5	63.4

[a] Average of theoretical values of carbons C(3) and C(3′)

[b] C(7) and C(8) of DPO indistinguishable under present experimental conditions

[c] All *s-trans* conformation

[d] All *s-cis* conformation

FIGURE CAPTIONS

FIGURE 1. Sample ^{13}C spectra of DPH dissolved in ZLI-1167. A: T=354K (isotropic); B: T=348K; C: T=332K D: T= 307K. The common scale is in relative p.p.m., referred to the position of the -CN peak of the solvent in the isotropic phase. Carbon assignments are also reported (see text).

FIGURE 2. Temperature dependence and assignments of the chemical shifts (p.p.m.) of BP in the isotropic and nematic phase of ZLI-1167, referred to the chemical shift of the -CN group of the liquid crystal in the isotropic phase. Nematic-isotropic temperature T_{NI} = 353K. Dashed lines connect the peaks belonging to the same carbon at the various temperatures. Carbon labeling is also reported.

FIGURE 3. The same as in Fig.2 but for DPE. T_{NI} = 351K. Carbons which are experimentally equivalent are marked with a overbar.

FIGURE 4. The same as in Fig.2 but for DPB. T_{NI} = 356K. Carbons which are experimentally equivalent are marked with a overbar. Both the *s-trans* and *s-cis* (grey) structures are shown.

FIGURE 5. The same as in Fig.2 but for DPH. T_{NI} = 352K. Carbons which are experimentally equivalent are marked with a overbar. Both the *all-s-trans* and *all-s-cis* (grey) structures are shown.

FIGURE 6. The same as in Fig.2 but for DPO. T_{NI} = 356K. Carbons which are experimentally equivalent are marked with a overbar. Both the *all-s-trans* and *all-s-cis* (grey) structures are shown.

FIGURE 7. Molecular frame embedded on the phenyl rings of each structure. The definition of the angle γ specifying the σ tensor principal axis is also shown.

FIGURE 8. Comparison between experimental and calculated isotropic chemical shift in ZLI-1167, relative to the chemical shift of carbon 1 of each structure. See figs. 1-5 for carbon labelings.

FIGURE 9. Crosses: reference benzene for carbons $1, \overline{2}$. Empty circles: reference ab initio for carbons $1, \overline{2}, \overline{3}, 4$. Shielding tensors for carbons $\overline{2}, \overline{3}$ taken as averages of carbons 2,2′ and 3,3′, respectively. The error bars are estimated by assuming that the shielding tensors of the reference carbons differs from true ones with a root-mean-square-deviation of 3 p.p.m. for the principal value components and of 2° for the orientation of the principal frame in the phenyl plane.

FIGURE 10. Order parameters $\langle D^2_{00} \rangle \equiv \langle P_2 \rangle$ (solid lines) and $\langle D^2_{02} \rangle$ (dashed lines) at three reduced temperatures $T* = T/T_{NI}$ in the nematic range: $T* = 0.99$ (circles), $T* = 0.93$ (diamonds), $T* = 0.88$ (squares). Full symbols correspond to order parameters derived from time-dependent fluorescence depolarization experiments and are taken either from Ref.[29] [71] (DPH) or Ref.[30] [72] (DPO)

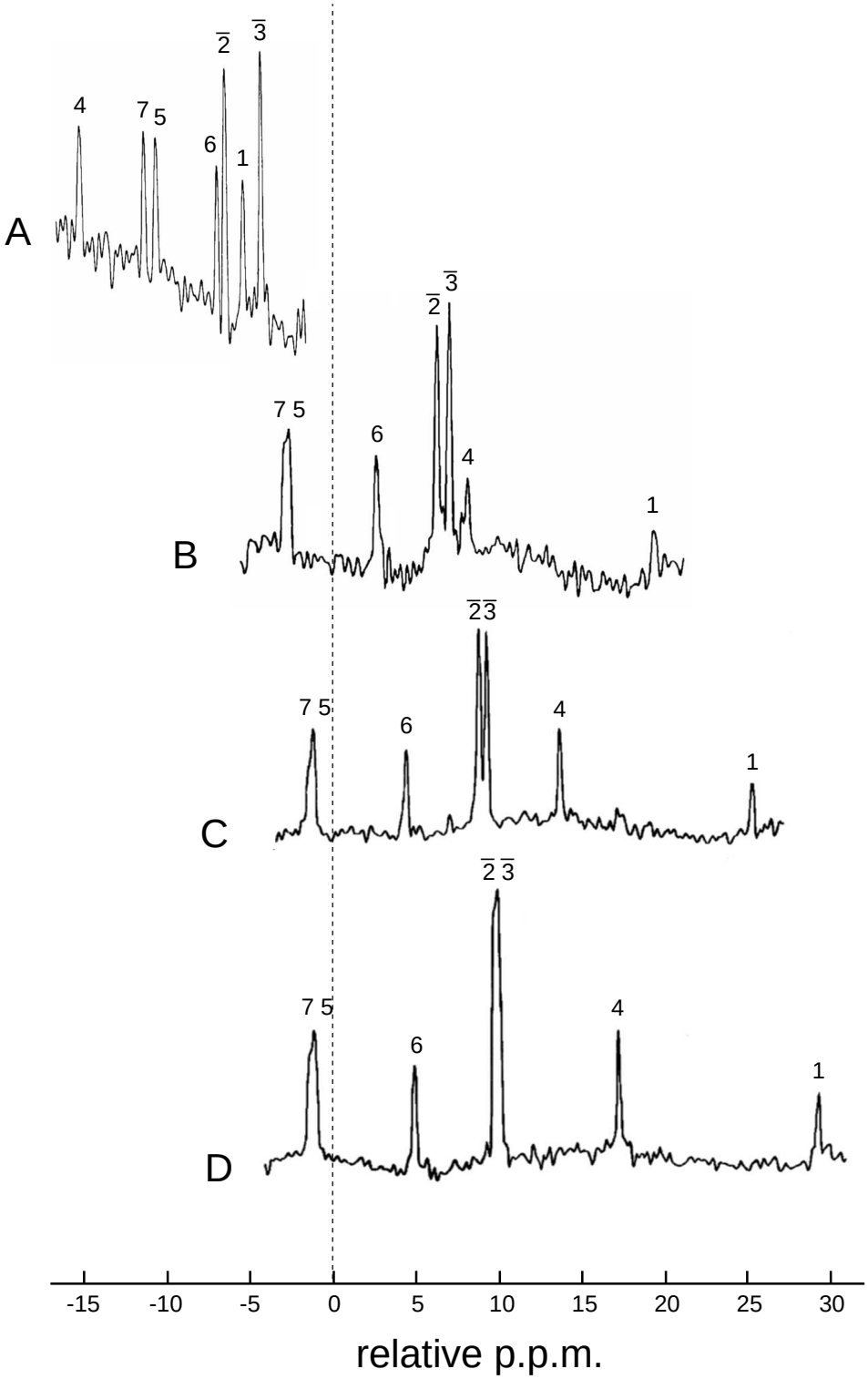

C. Benzi et al., FIG.1

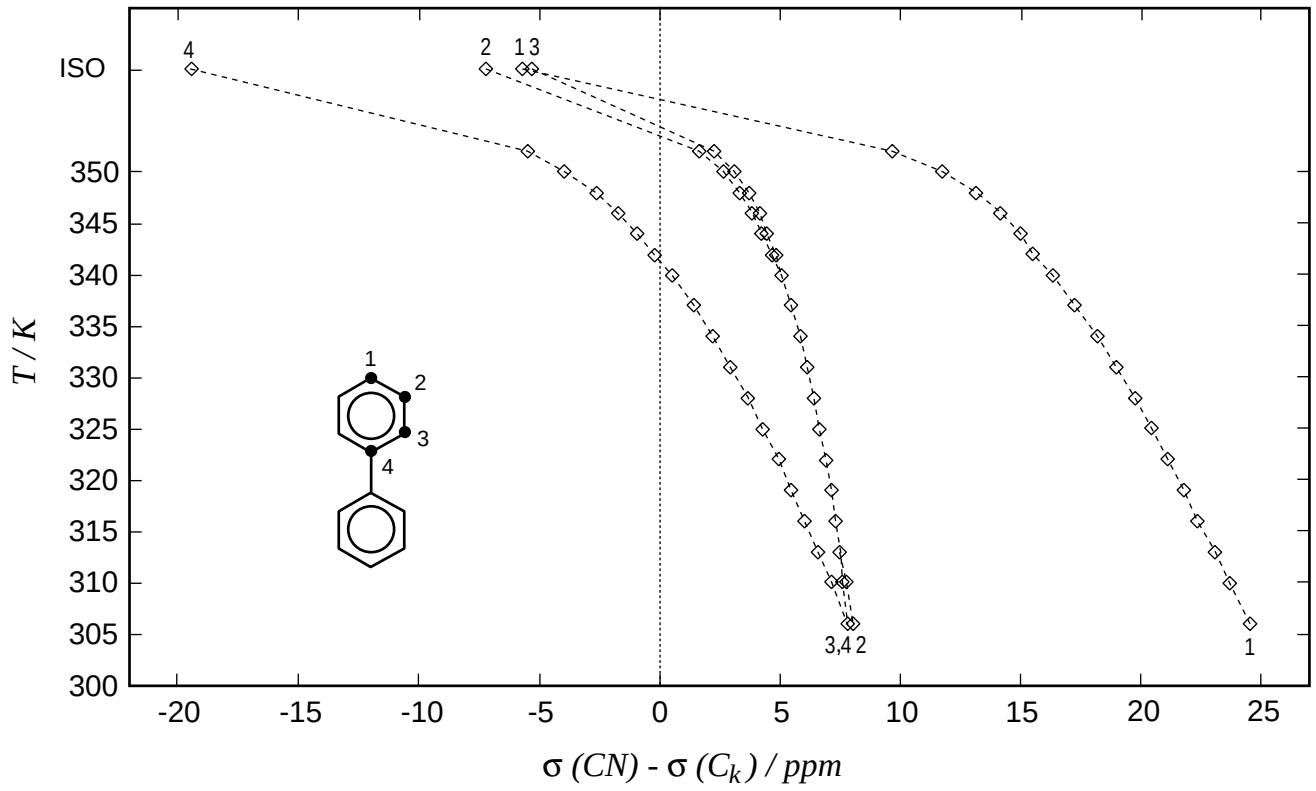

C. Benzi et al., FIG.2

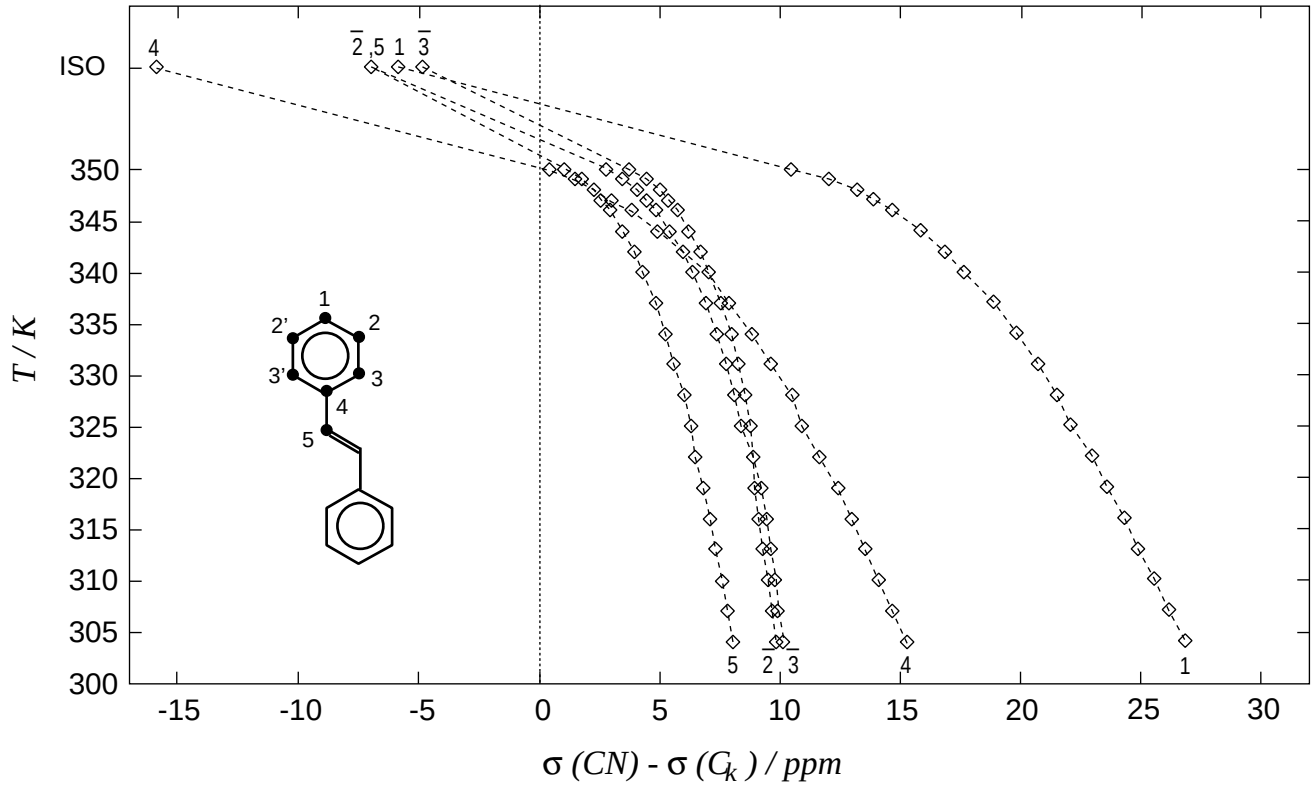

C. Benzi et al., FIG.3

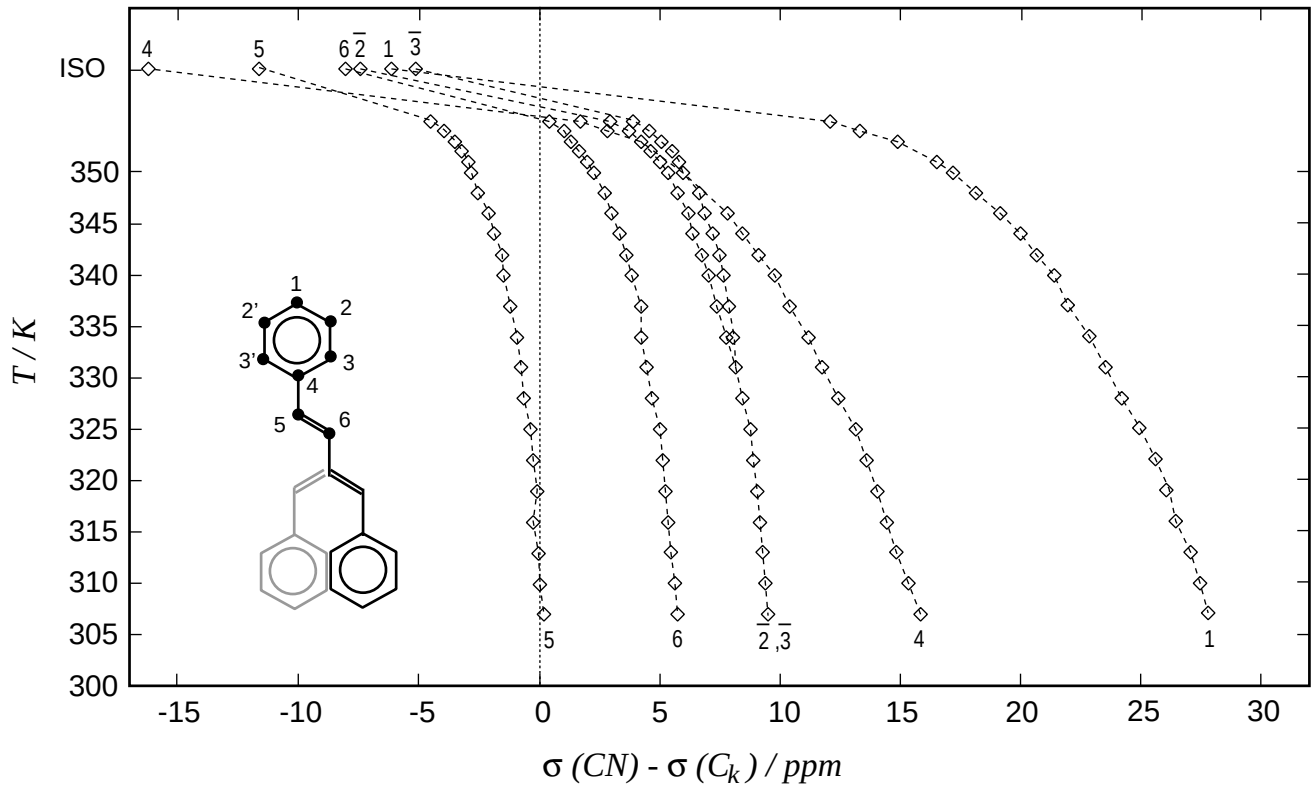

C. Benzi et al., FIG.4

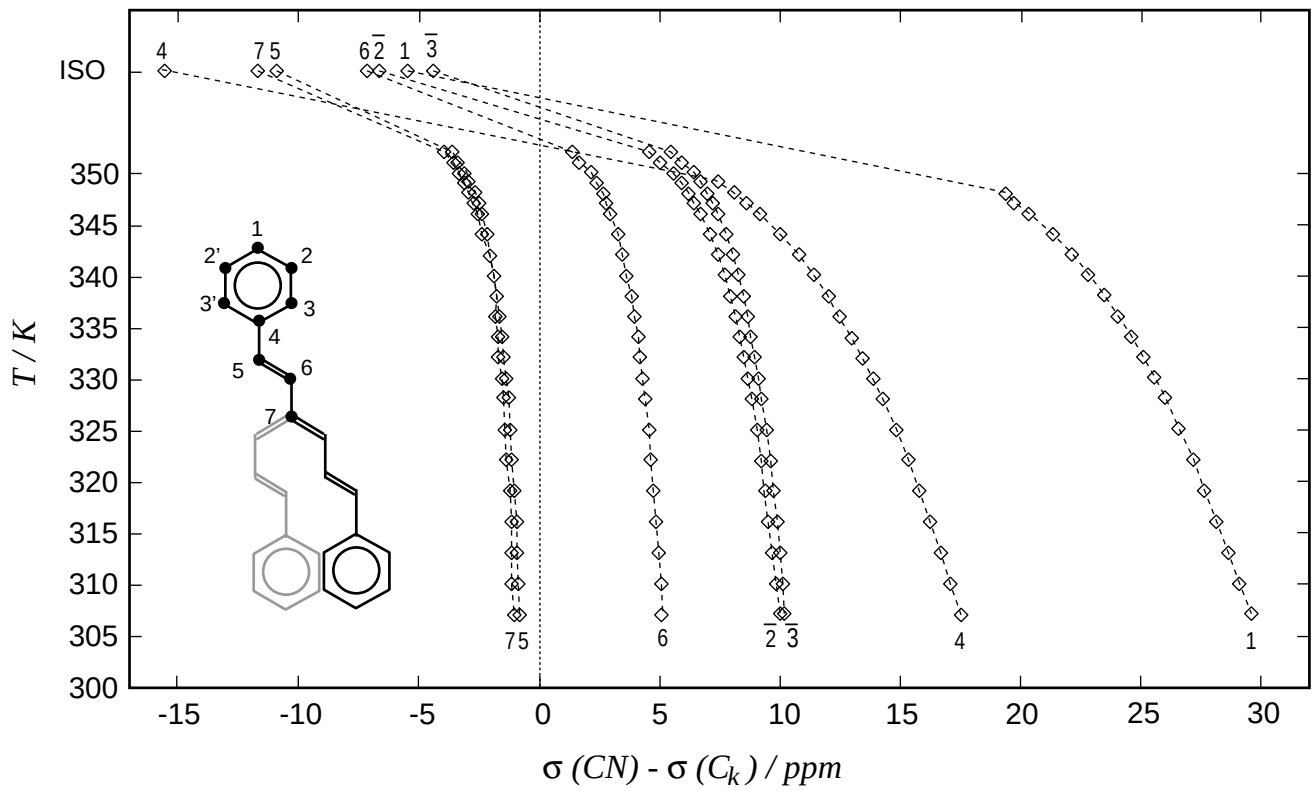

C. Benzi et al., FIG.5

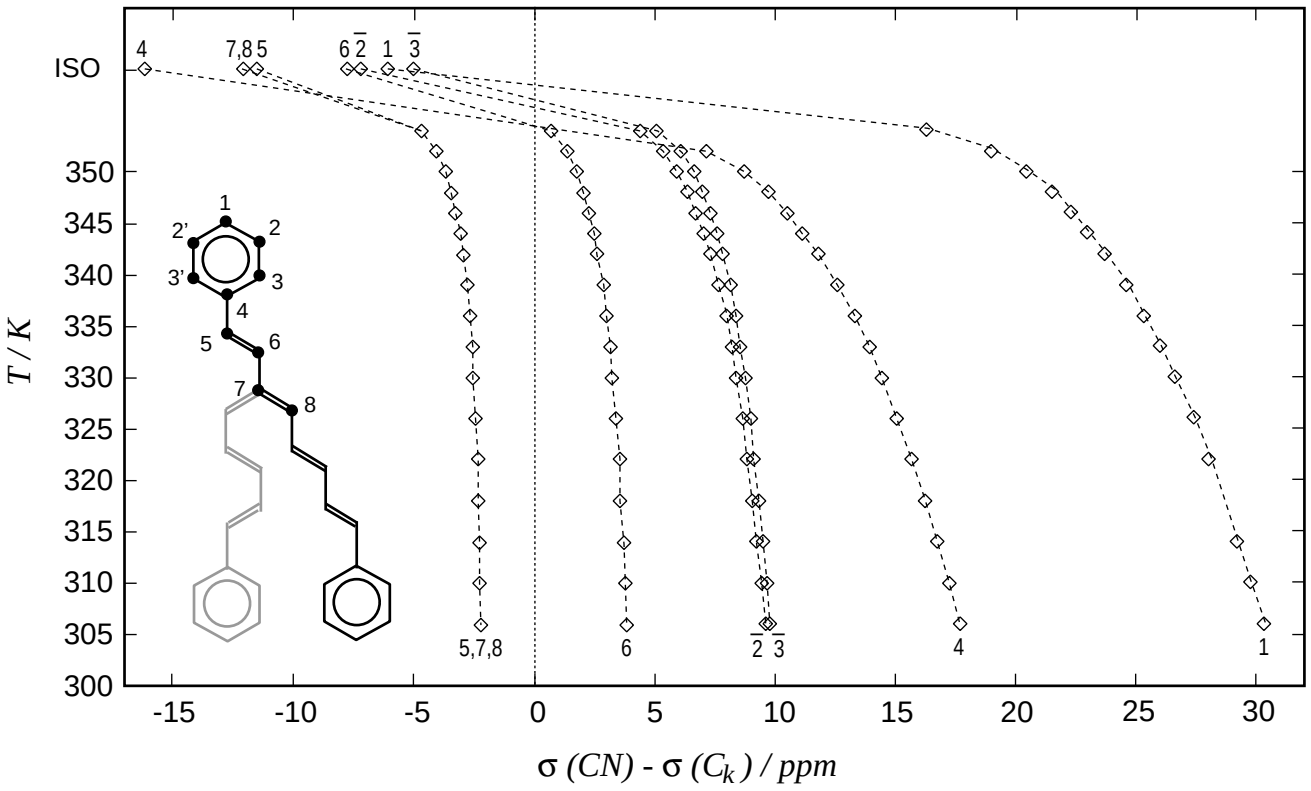

C. Benzi et al., FIG.6

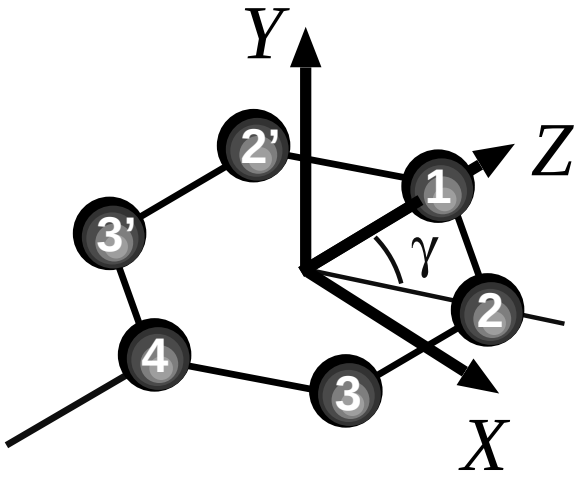

C. Benzi et al., FIG.7

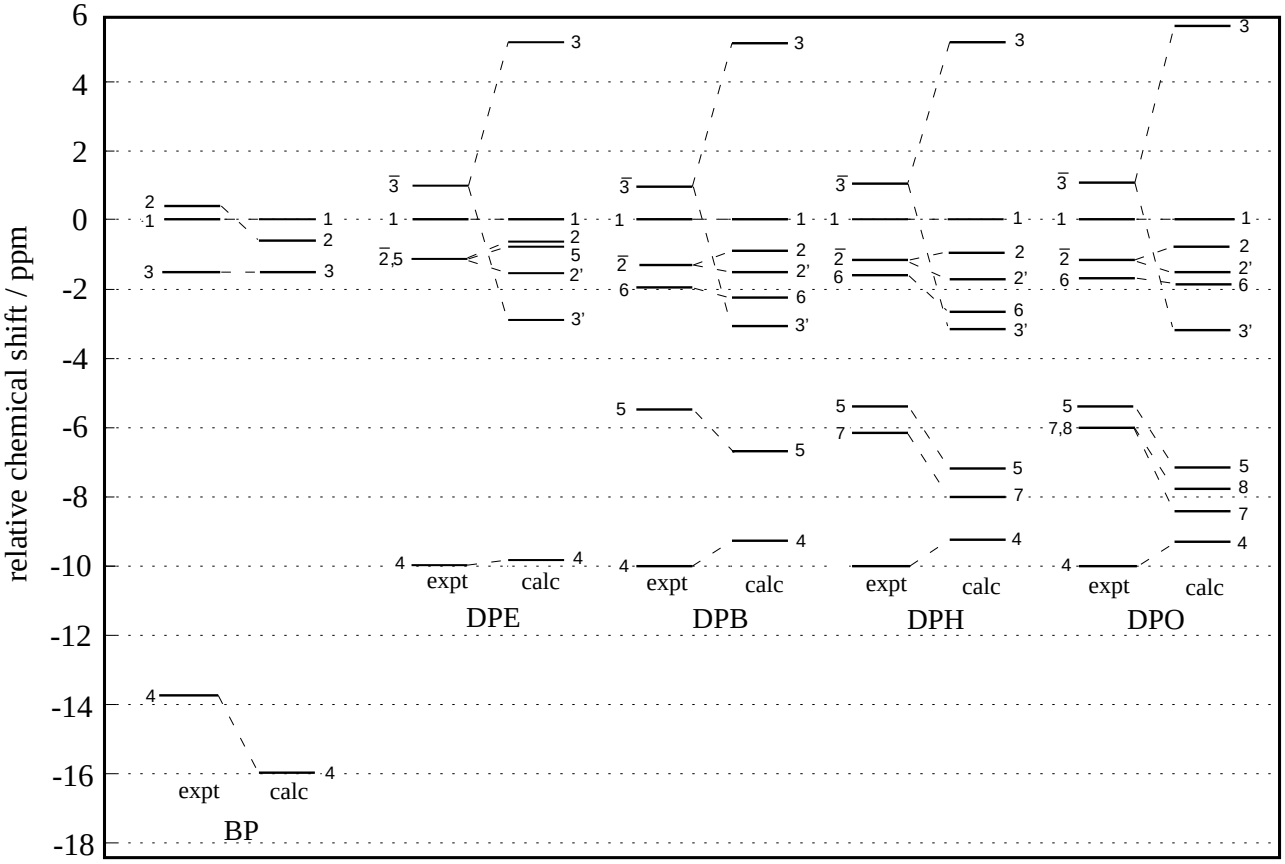

C. Benzi et al., FIG.8

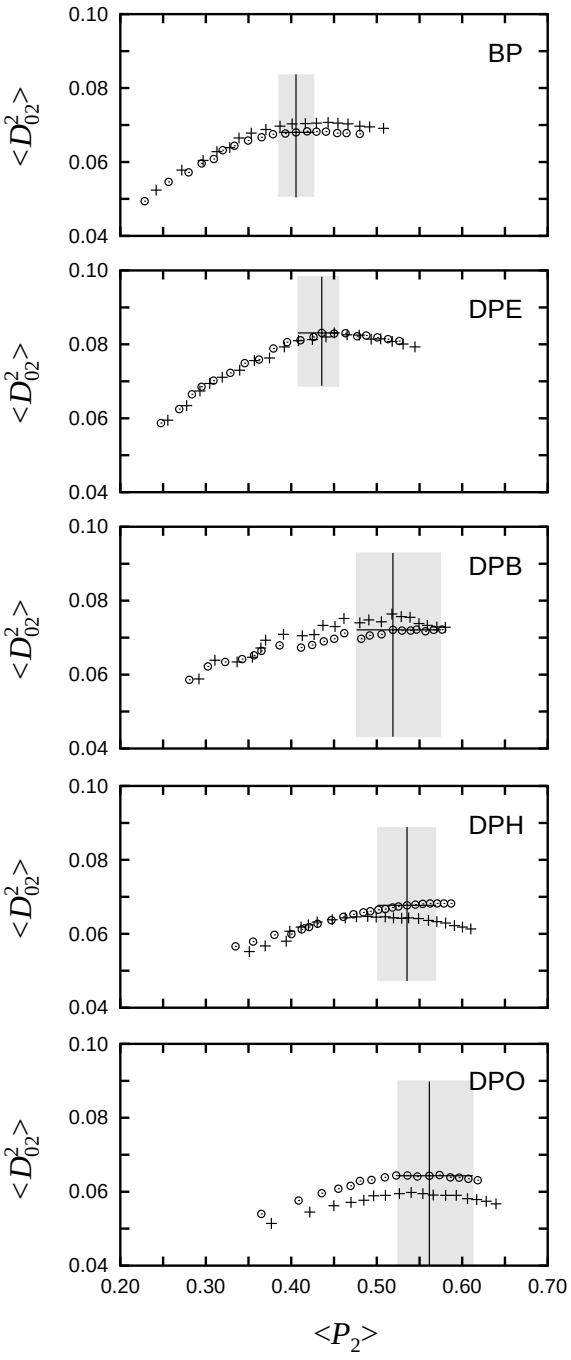

C. Benzi et al., FIG.9

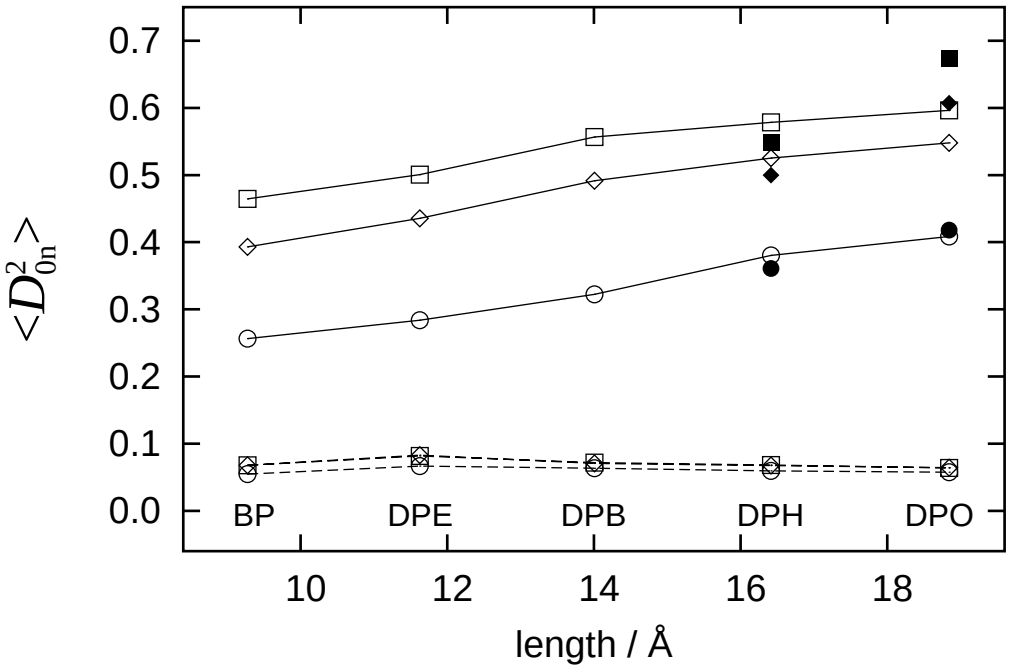

C. Benzi et al., FIG.10